Characterization by computed tomography of Ti64/20Ag composites fabricated by infiltration

V.M. Solorio[1], H.J. Vergara-Hernández[1], L. Olmos[2], D. Arteaga[3]

[1] TecNM/Instituto Tecnológico de Morelia, DEPI, 58120, Morelia, Michoacán, México.
[2] Universidad Michoacana de San Nicolás de Hidalgo, INICIT, 58060, Morelia, Michoacán, México.
[3] Universidad Nacional Autónoma de México, Blvd. Juriquilla No. 3001. Querétaro, 76230, México.

Aims

Although Ti6Al4V (Ti64) alloy presents excellent properties for use in medical devices, they cannot prevent bacterial infections. This can lead to bone damage by circumferential bone loss that may also compromise the joint with the implant. Thus, a reduced bone mechanical strength would in turn lead to failure of the implant [1]. In order to overcome this weakness, Ti alloys have been improved by adding a metal with antibacterial properties, such as Ag and Cu [2]. There are two points of view regarding the mechanisms of antibacterial action of the Cu and Ag metals. The first and widely accepted is the one related to the released metal ions killing bacteria, as it is considered that the dissolution of silver ions forms reactive oxygen species (ROS). ROS affect the DNA (as they oxidize and modify some cellular components and prevent them from performing their original functions), cell membranes and membrane proteins. The dissolution of silver ions may also cause free radicals on the titanium surface that destroy the bacterial structure and so generate the silver ion sterilization [3, 4]. The second one is related to the contact sterilization, it is considered that the presence of Ag particles on the surface of the metal can generate normal physiological metabolic disorders of bacterial cell membrane, thus, leading to bacteria death [5]. Shi et al. [6] demonstrated that the precipitation of Ti_2Ag in a contact sterilization mode plays a major role in the antibacterial ability of the Ti- Ag alloy than the silver ion release. Therefore, Ti64/xAg composites can be fabricated by liquid state sintering and casting. Since the Ag is immiscible with the Ti according to that reported before [7], the main objective of this work is to determine the feasibility to fabricate Ti64/Ag composites by the infiltration process. In order to verify the distribution of the Ag liquid in the Ti64 matrix a 3D image analysis is mandatory. For that, computed tomography is used for characterizing the distribution of Ag and Ti64 phase as well to determine the residual porosity that remains in the compacts after infiltration.

Method

In this work, spherical Ti64 powders with a particle size distribution between 45 to 75 µm were poured into a 3 mm diameter stainless steel die and then axially pressed at 450 MPa to fabricate cylindrical compacts of around 3 mm height. Then, the green compacts were sintered at 1100 °C during 5 min under inert atmosphere (high purity argon) in a vertical dilatometer. This is with the aim to fabricate a porous compact. According to Olmos et al. [8] Interparticle pores are fully interconnected for compacts with relative density lower than 85 %. After that, the relative density is calculated by measuring the volume of compacts and weighting them. The relative density was around 80 %, which means that porosity is 20 %. Next, the needed mass of Ag to fill the 20 vol.% of the compact is weighted and it is also poured into the same 3 mm die and axially pressed at 100 MPa to obtained a green disc of Ag. This is placed at the top of the Ti64 compact and then, introduced at the dilatometer, in where they are heated up to 1100 °C under Ar atmosphere. As the melting point of Ag is 960 °C, this temperature ensures that the liquid can

drain into the Ti64 porous compact. Finally, the sample was mounted in a Zeiss Xradia 510 Versa 3D X-ray microscope to acquire a 3D image. The beam intensity was set at 140 kV, which was high enough to pass through Ti6Al4V/20Ag composite, of around 3 mm diameter. 1600 projections were recorded around 360° of the sample with a CCD camera of 1024x1024 pixels. The quality of the images is good, which allows to segmented each phase by selecting the range of intensity in gray levels for each one, as detail by Garnica et al. [9]. This procedure allows to obtain binary images that corresponds to the interest phase, Ti64, Ag or pores, and the rest in black. From the binary images of each phase was possible to obtain different information, like volume fraction, connectivity and pore size distribution. The 3D image analysis procedure has been detailed by Olmos et al. [10]. In addition, a particle segmentation was performed by following the procedure reported by Vagnon et al. [11]. This allows to obtain information about the neck sizes between Ti64 particles, coordination number to locally evaluate the interaction between Ag and Ti64 phases.

Results

2D virtual slice of the transversal section of Ti64/20Ag composite is shown in Figure 1a. It is possible to distinguish 3 different intensity gray levels, light gray, dark gray and dark. According to the x-ray absorption, as the density increases the absorption does to. Therefore, lowest absorption is representing in black and correspond to the void spaces, it's means the pores. The second intensity gray level is the dark gray that corresponds to the Ti64 because its density (4.45 g/cm^3) is lower than the one of Ag (10.49 g/cm^3). This leads to the highest gray level has to be the Ag phase. As it can be observed from Figure 1a, the Ag fills the Interparticle voids left by the Ti64 particles that remains with spherical shape. In order to show the 3D connectivity, a 3D volume of each phase is rendered in Figures 1b, 1c and 1d. 3D images were rendered by a color code, in where a same color indicates that the volume is connected and different color indicates objects that are no connected with the rest of the image. As it was expected Ti64 and Ag phases are fully connected, this confirms that Ag fills the Interparticle pores left by the Ti64 particles. On the other hand, pores are fully isolated. This could indicate that such pores were isolated before infiltration or they are connected by small struts in where the liquid cannot penetrate.

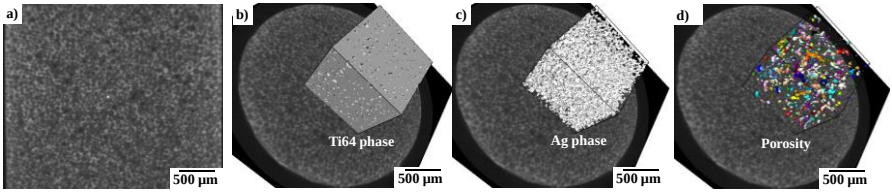

Figure 1. a) 2D virtual slice of transversal section of the Ti64/20Ag composite, b), c) and d) 3D inner volume rendering of the Ti64, Ag and pores phases, respectively.

To obtain quantitative data a representative volume (RV) was extracted from the center of the image, the RV was determined to be a volume of 300 voxels per side that represents a volume of 0.73 mm^3. A 3D rendering of the Ti64, pore and Ag phases is shown in Figures 2a, 2b and 2c, respectively. From this images it can be clearly notice that Ti64 and Ag phases are fully connected and the remaining pores are isolated and randomly distributed. The phase and pore size distributions were estimated by using the granulometry methodology and the cumulative distribution is plotted in Figure 3. The median size of the Ti64 particles is 74 µm (Table 1), which is in the range of the initial particle size distribution. The median Ag size is 25 µm that is a third of the Ti64 particles size. This values agrees with the pore size values reported by Olmos et al. [8] for copper powders sintered at similar values of relative density. This confirms that Ag filled the porosity left by the Ti64 particles. The distribution of Ag size goes from 7 to 50 µm,

meanwhile the one of Ti64 particles goes from 20 to 100 µm, Figure 4. The pore size distribution is a quite larger than the Ag with pores up to 55 µm and a median pore size of 36 µm, Table 1. The volume fraction of the Ti64 measured from 3D images corresponds well with the one measure by the volume and mass of the compact before infiltration, 80.2%. The volume fraction of the Ag is 17.2% and the porosity is 2.6%, which allows to obtain composites with lower porosity that is isolated and nearly spherical.

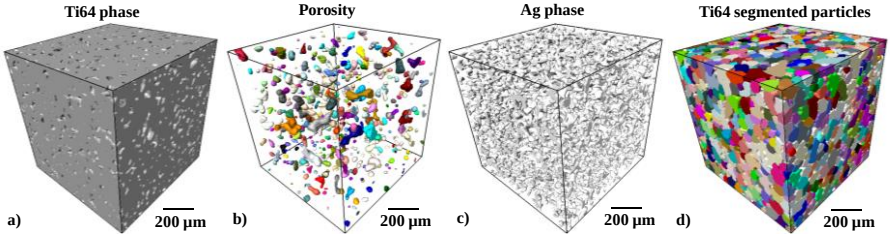

Figure 2. 3D rendering of; a) Ti64, b) Ag and c) pores phases, and d) 3D rendering of the Ti64 particles separated.

Table 1. Quantitative data extracted from 3D images of the Ti64/20Ag composite.

Phase	Volume fraction (%)	Median size (d_{50} µm)	Coordination number (Z)	Average (a/r)
Ti64	80.2	74	8.2	0.36
Ag	17.2	25	--	--
Porosity	2.6	36	--	--

Beside the global data, individual particle information can be obtaining from the 3D images with the Ti64 particles segmented, Figure 2d. Coordination number (Z) that gives information about the interaction between Ti64 particles is estimated for each particle in the 3D volume and the average value is listed in Table 1. The value of 8.2 is in the good range for powder compacts with similar relative densities reported elsewhere [8]. The ratio of the neck size and the particle radius (a/r) indicates the advancement of sintering and gives an idea of the mechanical resistance of the sintered compacts. To obtain this value, each contact between two particles is determined in the 3D volume. Next, the average radius of both particles in contact is calculated by assuming that particles are spherical. Then, the neck radius between those particles is calculated by assuming that neck is a cylinder with a height of 1 voxel. This is because the particle's separation procedure generates objects of 1 voxel thick. This is an idealized form of sintering that can be assumed to estimate the value since the Ti64 particles are nearly spherical. Finally, the average value of all contacts is calculated and listed in Table 1. The value of 0.35 corresponds to the intermediate stage of sintering that gives enough mechanical strength to withstand the stresses generated by the pressure of Ag liquid and conserve the initial shape. Figure 4a illustrates a Ti64 particle analyzed individually, in where the Ti64 particles in contact with it are in blue (Figure 4b), the necks between particles in contacts are in yellow (Figure 4d) and the Ag phase surround it in light grey (Figure 4c). Thanks to the computed tomography is possible to perform a detailed analysis that can bring information for the distribution of Ag after the infiltration process.

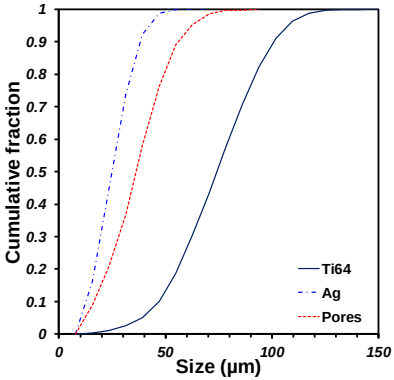

Figure 3. Size distribution of the Ti64, Ag and pore phases.

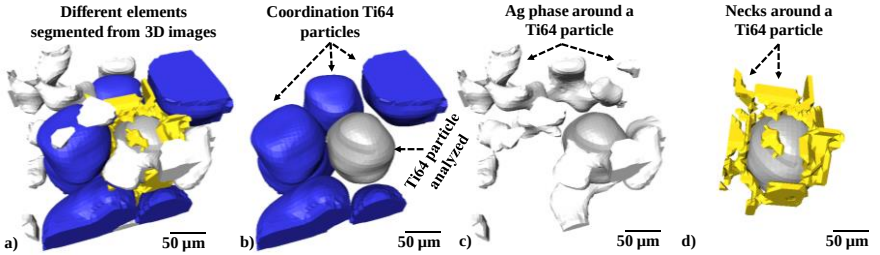

Figure 4. a) 3D rendering of a Ti64 particle surrounded by Ti64 particles in contact with it and necks developed among them and Ag liquid. b) coordination particles around a Ti64 analyzed particles, c) Ag liquid surrounded the analyzed Ti64 particle and d) necks developed during sintering between the contacting Ti64 particles.

Conclusion

Composites of Ti64/Ag fabricated by infiltration of the melt Ag were analyzed by computed tomography. Through the 3D image analysis was determined that Ag liquid can fill the Interparticle pores with a continuous phase surrounded the Ti64 particles. It was also observed that remaining pores are isolated and the volume fraction is low, 2.6%. Information about individual particles can be extracted from 3D images that can be used to get a deeper analysis of the mechanical properties of such kind of composites. It can be concluded that computed tomography is useful tool for characterizing the microstructure of composites.

References:

1. Zhang, E., Zhao, X., Hu, J., Wang, R., Fu, S., & Qin, G. “Antibacterial metals and alloys for potential biomedical implants” Bioactive materials, 6(8), 2569-2612, (2021).
2. Fu, S., Zhang, Y., Qin, G., & Zhang, E. “Antibacterial effect of Ti-Ag alloy motivated by Ag-containing phases” Materials Science and Engineering: C, 112266, (2021).
3. Marambio-Jones, C., & Hoek, E. M. “A review of the antibacterial effects of silver nanomaterials and potential implications for human health and the environment” Journal of nanoparticle research, 12(5), 1531-1551, (2010).
4. Li, M., Nan, L., Xu, D., Ren, G., & Yang, K. “Antibacterial performance of a Cu-bearing stainless steel against microorganisms in tap water” Journal of Materials Science & Technology, 31(3), 243-251, (2015).
5. Chen, M., Yang, L., Zhang, L., Han, Y., Lu, Z., Qin, G., & Zhang, E. “Effect of nano/micro-Ag compound particles on the bio-corrosion, antibacterial properties and cell biocompatibility of Ti-Ag alloys” Materials Science and Engineering: C, 75, 906-917, (2017).
6. Shi, A., Zhu, C., Fu, S., Wang, R., Qin, G., Chen, D., & Zhang, E. “What controls the antibacterial activity of Ti-Ag alloy, Ag ion or Ti2Ag particles?” Materials Science and Engineering: C, 109, 110548, (2020).
7. Nagase, T., Matsumoto, M., & Fujii, Y. “Microstructure of Ti-Ag immiscible alloys with liquid phase separation” Journal of Alloys and Compounds, 738, 440-447, (2018).
8. Olmos, L., Takahashi, T., Bouvard, D., Martin, C. L., Salvo, L., Bellet, D., & Di Michiel, M. “Analysing the sintering of heterogeneous powder structures by in situ microtomography” Philosophical Magazine, 89(32), 2949-2965, (2009).
9. Garnica, P., Macías, R., Chávez, J., Bouvard, D., Jiménez, O., Olmos, L., & Arteaga, D. “Fabrication and characterization of highly porous Ti6Al4V/xTa composites for orthopedic applications” Journal of Materials Science, 55(34), 16419-16431, (2020).